Optical Coherence Tomography and Optic Nerve Edema

9

Laurel N. Vuong and Thomas R. Hedges III

9.1 Papilledema

Information given to us by optical coherence tomography (OCT) has advanced our understanding of the pathophysiology of papilledema and pseudopapilledema. In 1860, von Graefe described engorgement and distention of the retinal veins as an early manifestation of papilledema, suggesting that increased intracranial pressure led to increased intracranial venous pressure and eventual venous stasis [1]. Subsequent investigators described dilatation of the optic nerve sheath in cases of papilledema, suggesting that increased pressure within the sheath could obstruct the central retinal vein [2, 3].

In 1963, in a study of rhesus monkeys, Hedges showed that, with acute and subacute increases in intracranial pressure, there was always an associated rise in ophthalmic vein pressure. He proposed that impairment of orbital venous outflow at the level of the cavernous sinus, arterial pressure elevation, and a local hemodynamic effects within the orbit all contribute to the elevation if orbital venous pressure [4]. In 1977, in an experimental model of rhesus monkeys, Tso and Hayreh demonstrated that, unlike swelling in the central nervous system which is characterized by fluid accumulation in glial cells and extracellular space, the primary pathologic change in papilledema is severe swelling of axons with disruption of mitochondria and neurotubules [5]. The Tso and Hayreh study also demonstrated that the edematous axons displaced the peripapillary retinal laterally, with extension of tracer into the subretinal space surrounding the optic nerve head. This idea of a direct communication between the swollen optic disc and the submacular space was first put forth by Samuel's histopathologic study in 1938, suggesting that the intermediary tissue of Kuhnt can be disrupted from optic nerve swelling with subsequent escape of peripapillary fluid [6]. Visual acuity loss, when it is seen in papilledema, is typically in conjunction with these macular changes [7].

L. N. Vuong (✉) · T. R. Hedges III
Tufts University School of Medicine, New England Eye Center, Neuro-Ophthalmology Service, Boston, MA, USA

A. Grzybowski, P. Barboni (eds.), *OCT and Imaging in Central Nervous System Diseases*, https://doi.org/10.1007/978-3-030-26269-3_9

Visual acuity loss is infrequent in papilledema. More commonly, chronic papilledema leads to degeneration of optic nerve fibers with resultant peripheral visual field loss [7]. In 1980, Morris and Sanders described visual acuity loss from papilledema due to macular changes, including retinal hemorrhages, macular exudates and choroidal folds. They suggested that cerebrospinal fluid pressure in the optic nerve sheath produces hemodynamic and mechanical effects causing compensatory dilatation of the retinal papillary and peripapillary plexus and distention of the optic nerve sheath, indenting the posterior globe causing choroidal and pigment epithelial wrinkling in the macula [8].

Shortly after, Corbett et al. showed that peripapillary fluid in the context of papilledema could lead to enlargement of the blind spot, hyperopia, and refractive scotoma [9]. In some patients with papilledema, macular retinal pigment epithelial changes, as seen in cases of chronic macular edema, have also been observed [10]. Even choroidal neovascular membranes have been described in patients with papilledema [11–19].

In 2001, Hoye et al. evaluated 55 patients with papilledema from increased intracranial pressure using time-domain OCT to measure the retinal nerve fiber layer (RNFL) thickness. Nineteen of the patients also had OCT of the macula during times of acute, subacute, or recurrent papilledema. OCT showed subretinal fluid in association with decreased visual acuity in a subset of patients. In some cases, this fluid was localized to the subfoveal region, and in others the fluid appeared to be continuous from the optic disc to the subfoveal region, suggesting fluid leakage from the optic nerve head. In these cases, fluorescein angiography, however, failed to demonstrate leakage from the retinal or choroidal vasculature. In cases in which the visual acuity was not substantially affected, there was thickening of the maculopapillary retina on OCT, suggesting intraretinal edema, without clear separation of the retina and underlying choroid. The authors further noted improvement in visual acuity after resolution of subretinal fluid [7].

A common clinical problem is the inability to clinically differentiate mild papilledema from pseudopapilledema. Although following these patients with repeated clinical examinations will eventually yield an answer, such action is subjective and could delay diagnosis.

In a study of patients under 20 years of age, time-domain OCT measurements of peripapillary RNFL thickness was found to be a reliable tool in assisting in the differentiation between frank papilledema and pseudopapilledema. The mean RNFL thickness in eyes with papilledema was 218% (340 μm versus 156 μm) thicker than the eyes with pseudopapilledema [20]. However, patients with moderate to severe papilledema can be readily distinguished from pseudopapilledema on clinical examination. Differentiating cases of *mild* papilledema from congenital crowding without optic disc drusen, however, is much more challenging. In 2005, Karam and Hedges showed that mean RNFL thicknesses, measured with a time-domain OCT, were significantly increased in patients with congenital crowding and mild papilledema in comparison to normal control patients. Although the patients with mild papilledema had higher RNFL values than those with congenital crowding, the difference was not statistically significant, and it was concluded that distinction between these similar appearing entities could not be made by OCT RNFL analysis alone. However, this

finding suggests pseudopapilledema and papilledema share a similar pathogenesis, in which axonal swelling is the result of delayed axoplasmic transport [21].

Fard et al. studied 42 eyes with mild papilledema, 37 eyes with pseudopapilledema from congenitally crowded discs, and 34 normal eyes with spectral-domain OCT (SD-OCT). Patients with optic disc drusen, moderate to severe papilledema, atrophic papilledema, and previous retinal disease were excluded. As previously found, eyes with both papilledema and pseudopapilledema had statistically significant increased RNFL thickness in comparison to normal subjects. In addition, the authors measured the peripapillary total retinal volume, which they defined as a volumetric region between the inner limiting membrane and the outer aspect of the retinal pigment epithelial complex in a defined space circumferential to the optic disc. Two peripapillary total retinal volumes were calculated as volumes (inner versus outer), from ring-shape areas concentric to the optic nerve. They found that the difference between the average outer peripapillary total retinal volume in the papilledema and pseudopapilledema groups was statistically significant. However, the difference between the outer ring peripapillary total retinal volume in pseudopapilledema and normal eyes was not. They concluded that outer peripapillary total retinal ring volumes might be useful in helping to differentiate between papilledema and pseudopapilledema [22].

Kupersmith, Sibony, and et al. have used OCT in a different manner to try to distinguish papilledema from other types of optic disc edema. In 2011, the authors published two articles studying the biomechanical changes of the optic nerve head in patients with papilledema secondary to elevated intracranial pressure, optic neuritis and non-arteritic anterior ischemic optic neuropathy (NAION). Specifically, the authors measured the angle of the peripapillary retinal pigment epithelium and Bruch's membrane (pRPE/BM) at the temporal and nasal borders of the neural canal opening. The angle was measured as positive with inward (toward the vitreous) angulation and as negative with outward angulation (away the vitreous) amongst the patients in the three categories. Only OCTs from patients with papilledema showed a positive angulation. Since, the same angulation was not seen in NAION or optic neuritis, the angulation was concluded to be secondary to elevated intracranial pressure [23, 24]. A follow-up study by Sibony et al. [25] and data from the idiopathic intracranial hypertension treatment trial [26], showed that the pRPE/BM positive angulation in patients with papilledema became more negative as the intracranial pressure decreased through any means, thus confirming their previous conclusion. Interestingly, Sibony et al. also found the same positive angulation in patients with presumed optic nerve sheath meningioma. While the authors were uncertain of the mechanism, they postulated it might involve a change in the compliance of the nerve or localized sequestration of cerebrospinal fluid in the distal optic nerve sheath or a combination of both [27].

OCT has also been valuable in demonstrating the natural history of optic disc edema from a variety of causes by measuring the RNFL thickness. OCT can objectively quantify the amount of RNFL swelling, and thus axonal swelling, which is the main pathological event in optic nerve edema; conversely, confocal scanning laser ophthalmoscope cannot due to disruption of mitochondria and neurotubules in the swelling axons [5, 28]. OCT can thus be an objective tool in following the clinical course of optic disc edema. After the period of acute edema, during which the RNFL is diffusely thickened, OCT can be used to monitor resolution of axonal

swelling and thinning of the RNFL. Long term, RNFL thinning on OCT can be used to monitor for evolution towards optic atrophy [28].

Monteiro and Afonso analyzed SD-OCT findings in patients with pseudotumor cerebri with clinically resolved papilledema and stable visual fields for at least 6 months. They found that macular and RNFL thickness measurements were significantly reduced when compared with normal eyes, and that the degree of RNFL and retinal axonal loss correlated with visual field loss. This study highlights that OCT can be used as an objective tool in guiding management and may estimate axonal loss following chronic papilledema [29].

The retinal nerve fiber layer is composed of the unmyelinated axons that originate from ganglion cell bodies in the macula [30]. Therefore, degeneration of the RNFL may lead to decreased average macular thickness reductions, at least in part secondary to ganglion cell death from retrograde axonal degeneration [31].

Papchenko et al. demonstrated a robust association between visual field sensitivity using automated perimetry and structural changes in OCT macular thickness in patients with NAION, suggesting macular thickness could be a surrogate for determining the extent of neuronal damage in non-glaucomatous optic neuropathy. Further, there was a topographical correlation between regions of macular thinning with corresponding visual field loss [32].

Average macular thickness measurements are the summation of multiple layers of the macula, including diverse cell types with diverse functions. However, recent advancements in segmentation algorithms have made it possible to measure some discrete retinal layers. Quantification of the retinal ganglion cell layer in the macula, therefore, may provide a more specific assessment of a discrete retinal neuronal population. Analysis of the ganglion cell layer complex (GCC), which is a combination of the ganglion cell and inner plexiform layers, in the macula has become an important tool in assessing various optic neuropathies [33–35].

Marzoli et al. showed that measurements of GCC thickness correlated better with decreases in visual field mean deviation than RNFL measurements in papilledema. They concluded that mean GCC thickness measurements give a more reliable estimate and an objective estimate of early retrograde optic nerve damage even in cases without papilledema or visual loss [36]. The NORDIC trial, which included patients with idiopathic intracranial hypertension (IIH) with mild visual fields loss, showed a correlation between the GCC measurements below the control fifth percentile and higher mean deviations on visual fields. Correlations were not seen with mean deviations and increased RNFL thickness [37]. Chen et al. reviewed the OCTs of 31 IIH patients in a retrospective study to determine the prognosis of visual acuity loss at initial presentation. Using a custom programmed analysis software, they found GCC thickness was a reliable objective measurement in predicting visual outcome [38]. Athappilly et al. [39] studied IIH patients with significant papilledema and vision loss (RNFL thicknesses greater than 200 μm and an average mean deviation on initial visual fields of −9.0). GCC analysis generated from commercially available software showed evidence of optic nerve injury as early as the first follow-up visit. Despite the presence of papilledema, GCC, in contrast to RNFL, was found to be a more reliable indicator of optic nerve injury and predictor of symptomatic vision loss. It was suggested that close follow-up and, if necessary, more aggressive management when GCC thinning is present could halt, or even reverse visual field loss.

The authors found that in cases where the RNFL thickness was greater than 200 μm, GCC analysis was not always reliable, presumably because of axon swelling as well as subretinal and intraretinal fluid obscuring the GCC (Fig. 9.1).

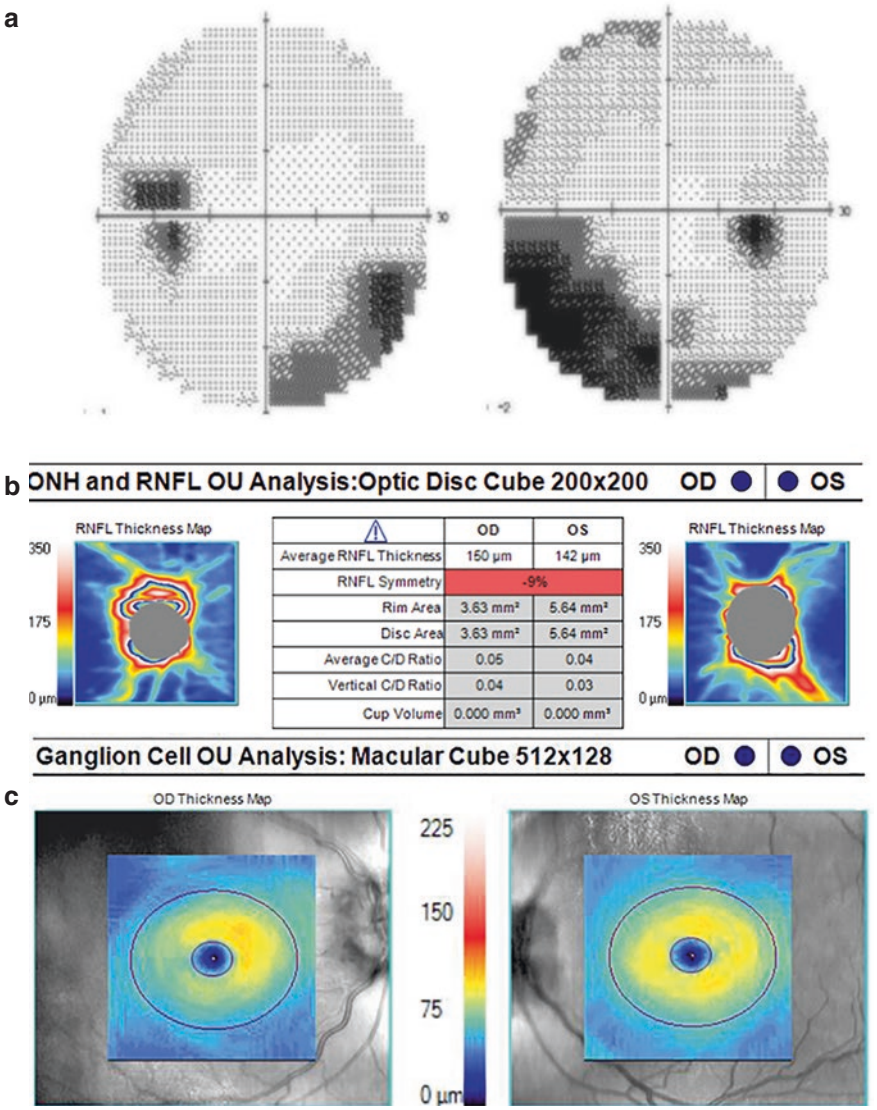

Fig. 9.1 A 33-year-old man with idiopathic intracranial hypertension treated with daily acetazolamide and optic nerve sheath fenestration in both eyes 5 years prior presented with blurred vision in both eyes and headache. There was moderate papilledema on fundoscopy and visual field examination revealed inferior arcuate scotomata in the right and left eyes (**a**). OCT demonstrated diffuse thickening on the RNFL bilaterally (**b**). Ganglion cell layer complex (GCC) analysis revealed segmental thinning, despite the papilledema (**c**). The opening pressure was elevated on lumbar puncture, and he underwent left transverse sinus stenting. Post stenting, his visual field examination remained largely unchanged in the right and left eyes (**d**). Although the optic disc swelling significantly improved (**e**), segmental GCC loss remained apparent in (**f**)

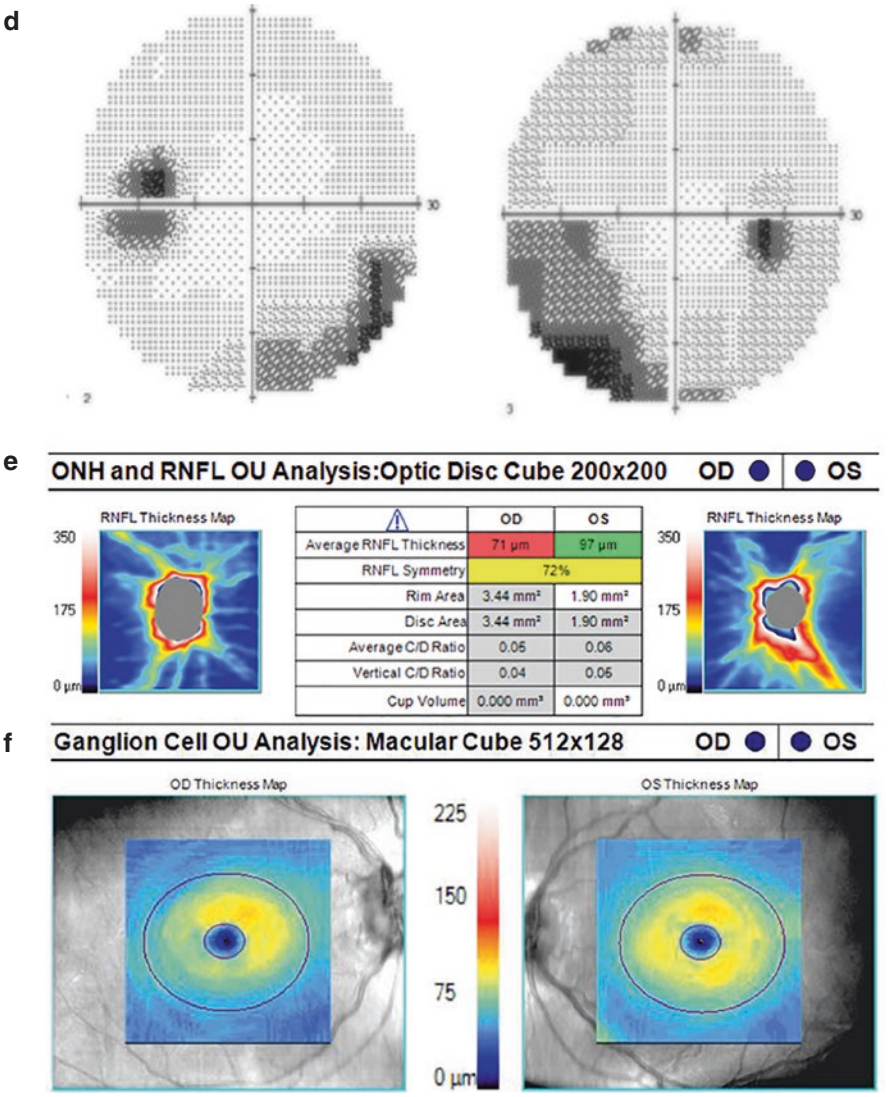

Fig. 9.1 (continued)

9.2 Optic Disc Edema Secondary to Ischemia

Non-arteritic anterior ischemic optic neuropathy (NAION) is characterized by abrupt visual loss with associated optic disc edema [40]. It is believed to be secondary to disrupted blood flow in a disc with retinal nerve fiber crowding and minimal to no physiologic cup. Although typically occurring unilaterally, optic disc edema secondary to NAION can be confused with papilledema resulting from increased intracranial pressure. Both conditions have been associated with axonal swelling and

axoplasmic flow stasis in the optic nerve head and can appear similar on ophthalmoscopy with disc swelling, obscured disc margins, and peripapillary hemorrhages [41].

NAION occurs acutely, and is followed by a period of axonal swelling and subsequent thinning. After atrophy of the retinal ganglion cells has occurred, the optic neuropathy remains relatively stable [28].

OCT can detect RNFL edema in NAION. In the acute phase, the RNFL of the involved eye is significantly thicker than the fellow eye, and can be nearly doubled [42–44]. The mean RNFL from superior, inferior, temporal, and nasal quadrants have been shown to all be significantly higher than the corresponding normal values [6]. This corresponds to histopathologic studies [45–48].

Over time, the optic disc edema decreases, and the RNFL undergoes thinning, corresponding to progressive optic atrophy and pallor. OCT can follow this evolution of initial thickening and progressive thinning of the RNFL as a proxy for estimating optic disc damage. By 2 months after the NAION event, the RNFL thickness is similar to the fellow eye, marking resolution of optic disc edema. By 3–4 months, RNFL thickness is decreased nearly 40% in comparison to the fellow eye. By 12 months, the retinal nerve fiber loss is typically stabilized, with only a 6% further reduction in RNFL thickness [42, 43]. Resolution of optic disc edema from the onset of visual acuity loss may be longer in patients with diabetes and maybe shorter in patients with worse initial visual field and visual acuity loss. Resolution of edema may be quicker in patients with more severe vision loss because the greater destruction of axons results in fewer axons to swell and cause edema [44].

Bellusci et al. used OCT to detect different patterns of RNFL damage in 16 eyes with NAION, classified by visual field (VF) loss. They found that eyes with NAION and VF loss limited to the inferior hemifield had RNFL atrophy limited to the superior half of the optic nerve head. Patients with diffuse VF loss had diffuse RNFL atrophy involving all quadrants around the disc. Patients with central or centrocecal scotomas had RNFL atrophy limited to the superior and temporal sectors [44]. Alasil et al. found a similar correlation between the peripapillary nerve fiber layer thinning on OCT and the severity and location of visual field defects. They also showed that the division between affected and nonaffected hemispheres is more complicated than the altitudinal defects seen on visual field testing, illustrated by the greatest relative loss of RNFL to be in the superior quadrant and superotemporal octant, correlating with visual field loss greatest inferonasally [49].

OCT demonstrates that some patients with optic disc edema secondary to NAION develop subretinal fluid, similar to that which occurs in papilledema [7, 50]. Hedges et al. found 8 out of 76 patients with NAION had subfoveal fluid when examined within 4 weeks of developing acute vision loss. Additional patients had peripapillary subretinal fluid and peripapillary subretinal fluid extending toward, but not involving, the fovea. OCT findings in the patients with subfoveal fluid included peripapillary subretinal hyporeflectivity adjacent to the elevated optic nerve head with retinal nerve fiber thickening and hyporeflectivity under the fovea. Decreased visual acuity corresponded to degree of macular thickening. Similar to the subretinal fluid reported in some patients with papilledema, in half of the NAION patients with subretinal fluid, the fluid appeared to extend from the optic disc to the fovea.

The other half of the patients had subretinal fluid in the peripapillary region and a separate area of subfoveal fluid. Reduction in OCT RNFL thickness and resolution of subretinal fluid corresponded to improvement in visual acuity [50].

Optic disc edema as demonstrated by increased RNFL thickness on OCT has limited prognostic value in patients with NAION; it is not correlated with final RNFL thickness, visual acuity, or visual field mean deviation. In non-glaucomatous optic neuropathies, like NAION, greater damage occurs in the papillomacular fibers, with resultant loss of central acuity. Therefore, although the site of damage occurs at the optic nerve head, axons have cell bodies in the macula and contribute to macular thickness [51]. Papchenko et al. studied the macular thickness in addition to the retinal nerve fiber layer thickness in patients with NAION, and found a stronger correlation between macular thickness and Humphrey visual field sensitivity than RNFL parameters, suggesting that macular thickness may be a surrogate marker for determining the extent of nerve injury in NAION. They found that in patients with inferior visual field defects, the total macula thickness and temporal thickness were thinner when compared to control eyes [32]. Similarly, Fernandez-Beunaga et al. found that nasal macular thickness correlated with visual acuity in ischemic optic neuropathy [51].

When it became possible to measure the GCC directly, Aggarwal et al. showed a high correlation of GCC thickness with visual field losses in both magnitude and location in patients with NAION, with hemispheric GCC loss correlating with altitudinal visual field loss [33]. Larrea et al. showed a significant correlation between GCC averages at the onset of NAION and visual field losses in both acute and chronic stages, suggesting that GCC thickness in the acute stage may be a determining factor to predict final visual field defects, with good correlation between location of damage in the GCC in the macular region and location of the scotoma [34].

Erlich et al. compared the pattern of GCC loss between NAION and patients with optic neuritis at time points less than 2 weeks from onset of symptom, 5–8 weeks, 9–16 weeks, and greater than 16 weeks and found there was a significantly greater hemispheric difference in GCC thickness in NAION patients than optic neuritis at every time-point measured [52]. However, the GCC hemispheric difference in NAION lessened at time points greater than 16 weeks. This may be explained by the observation that ganglion cell atrophy extends to a greater area, beyond one hemisphere, with time. The initial segmental ischemia of the optic nerve is associated with edema, which may lead to subsequent damage in other areas of the optic nerve [53, 54] (Fig. 9.2).

In early studies using OCT angiography (OCTA) to analyze the microvasculature of the retina and choroid nerve in NAION patients, flow impairment of the retinal peripapillary capillaries and peripapillary choriocapillaris was found to correspond with changes seen in the OCT measurements of the retinal nerve fiber layer and ganglion cell layer complex and to visual fields defects [55]. Comparison of acute and chronic NAION showed vessel density was significantly less in chronic NAION. No difference was seen in the microvasculature of the unaffected fellow eye of patients with NAION when compared to normal eyes. These findings suggest that OCTA may be a usual tool in diagnosing NAION and monitoring the course [56].

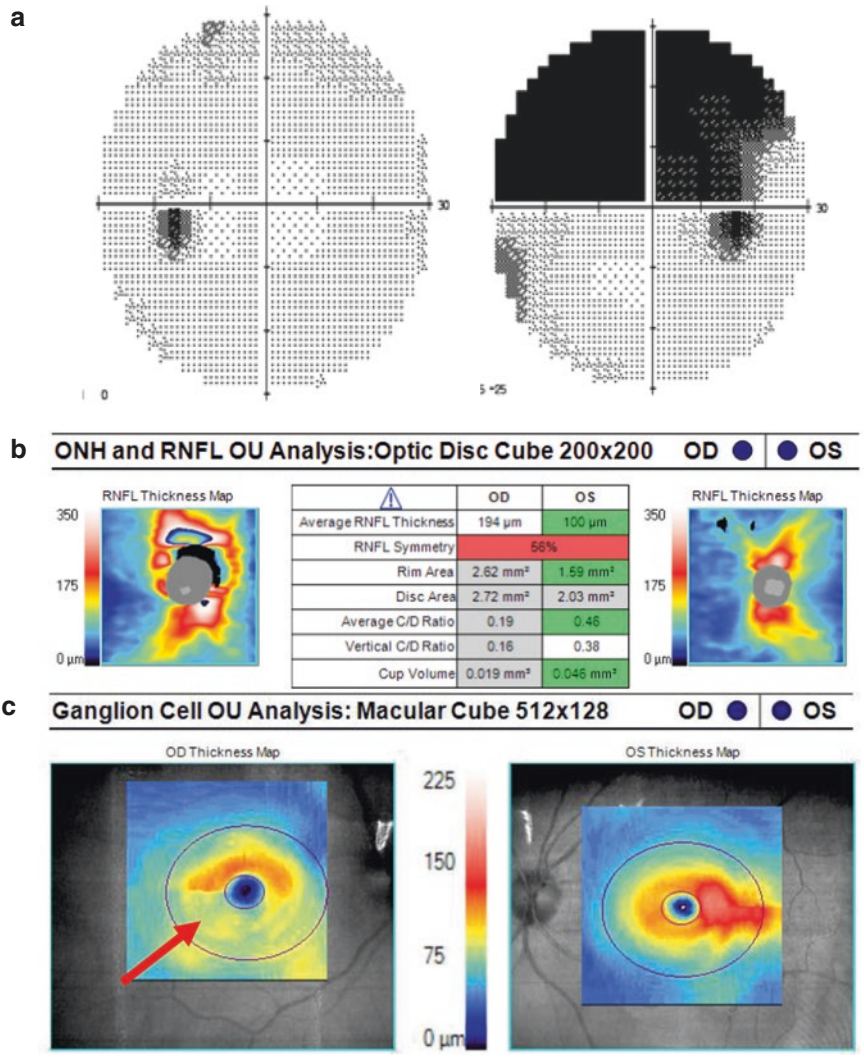

Fig. 9.2 A 78-year-old man with hypertension awoke with a dark shadow in his right eye upon awakening. Humphrey visual fields showed a superior altitudinal visual field defect OD and the visual field was full OS (**a**). Fundoscopy and OCT RNFL analysis showed diffuse swelling of the optic nerve in the right eye (**b**). Despite the edema on RNFL analysis, there was thinning inferiorly in the right eye on ganglion cell layer complex (GCC) analysis, suggesting neuronal loss (**c**). Two months later, the RNFL measurement normalized (**d**) in the right eye and GCC showed thinning, inferior greater than superior (**e**)

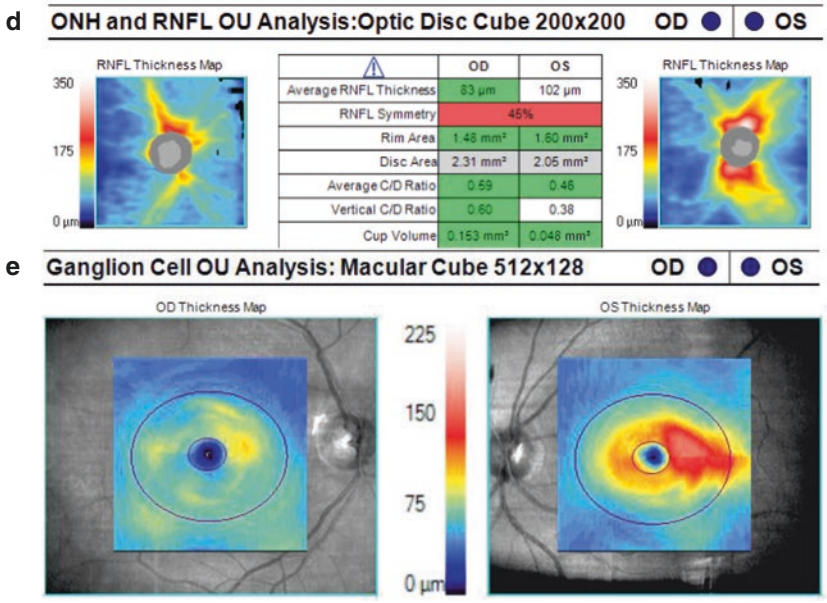

Fig. 9.2 (continued)

9.3 Optic Disc Edema Secondary to Toxic/Hereditary/ Nutritional Optic Neuropathies

SD-OCT has shed some light on the events occurring at the optic nerve head in Leber Hereditary Optic Neuropathy (LHON), including a clearer depiction of axonal swelling, which precedes and is present at the time of visual loss. Furthermore, OCT clearly shows, and can be used to measure, atrophy of the nerve fiber layer (RNFL) following the acute event, which in most cases, is confined to the papillomacular bundle [57–59]. Hedges et al. found that in the early phases of LHON, when visual acuity begins to decline, the GCC remains relatively normal, while the RNFL becomes swollen and is frequently associated with peripapillary telangiectasias. Within days, as the vision further declines, the GCC starts to thin. The RNFL thickening resolves or becomes thin only until the chronic phase in most patients. In some cases, average RNFL thickness remains relatively normal despite GCC loss, creating a mismatch between RNFL and GCC thickness measurements. In cases where RNFL loss is mild, the papillomacular bundle is affected. The degree of GCC thinning or RNFL loss does not correlate with final visual acuity or visual fields even if there is visual recovery [60] (Fig. 9.3).

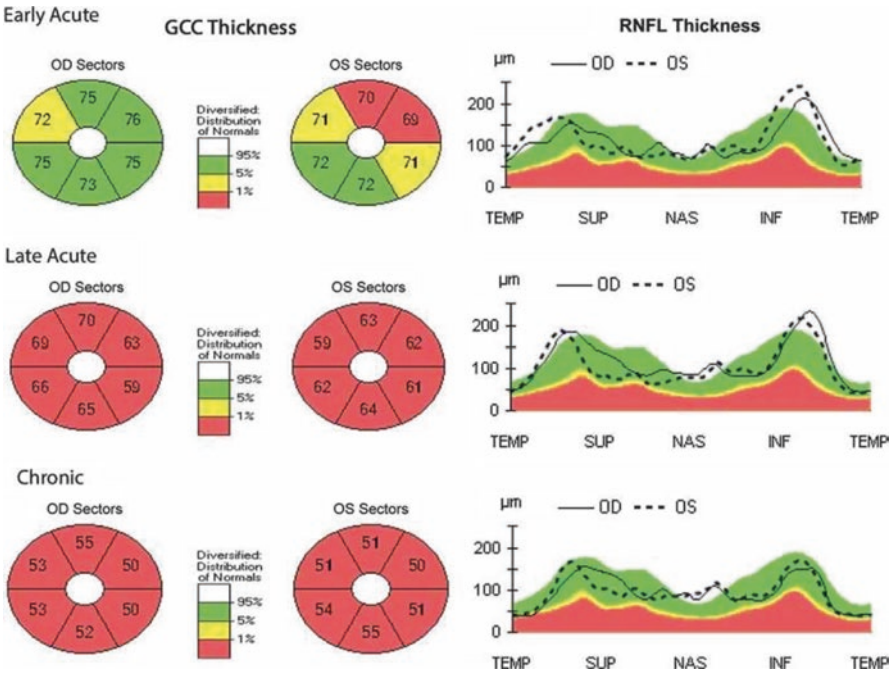

Fig. 9.3 OCT findings throughout the early acute, late acute, and chronic phases in a 44-year-old woman LHON with 11,778 mutation. She had decreased vision bilaterally (20/30 and 20/50) 3 weeks after symptom onset. In the early acute phase, ganglion cell layer complex (GCC) defects are noted bilaterally with RNFL swelling. In the late acute phase, severe GCC thinning is present with persistent RNFL swelling. In the chronic phase, severe GCC thinning is present with RNFL thinning noted temporally

In a handful of case reports using OCTA to evaluate LHON, results have shown that there is temporal radial peripapillary capillaries (RPC) thinning, in the papillomacular bundle, associated with LHON [61, 62]. Matszuki et al., were able to follow a patient with acute symptoms in one eye and pre-symptomatic in the other. They found that the RPC thinning and its spread did not precede the symptomatic vision loss. The authors suggest that based on this finding that it is reasonable to assume the spreading of the RPC less was a secondary association of RNFL thinning [62].

Barboni et al. analyzed the OCT RNFL and GCC thicknesses of patients with dominant optic atrophy (DOA) diagnosed with a mutation in the OPA1 gene and found that, overall, DOA patients have thinner RNFL and GCC measurements compared to age matched healthy subjects. The temporal RNFL was particularly thin regardless of patients' visual acuities. Inferior and superior quadrants of the RNFL

were thinner in the DOA patients with the worse visual acuities compared to those with milder vision loss. While, the GCC thinning was mostly similar despite different visual acuities, further analysis did show significant thinning in the superotemporal and superior sectors in the patients with visual acuities between 0.6–1.0 and 0.4–0.5 [63].

In a small case series of three patients, Moura and Monteiro found that 2 of their patients with a chronic history of vision loss related to excessive alcohol intake and cigarette smoking showed temporal RNFL thinning using time-domain OCT. The third patient, whose vision loss had only been present for half of year, very mild temporal RNFL loss in one eye, but overall the RNFL was thick [64]. Kee and Hwang, published a case report of one patient with progressive vision loss over the course of 4 years who had a similar RNFL pattern of thinning and thickening. Increased RNFL thickness was found to be consistent with OCT findings in a case of methanol poisoning with severe peripapillary nerve fiber swelling and intraretinal fluid accumulation [65], and may be explained with pathologic findings of mitochondrial swelling and vacuolation in the retinal pigment epithelium, photoreceptor inner segments, and optic nerve verified in a rodent model [66, 67]. Klein et al. showed nasal GCC thinning in one patient who presented 1 month after bilateral decreased vision from methanol and then in follow-up 8 months later. The selective involvement of the papillomacular bundle fibers is common in toxic optic neuropathies and represents damage to the small caliber axons rich in mitochondria. Despite severe systemic toxicity, the relative sparing of the optic nerve in this case enabled characterization of the evolution of methanol toxicity with segmental GCL involvement and preservation of the RNFL, corresponding to the papillomacular bundle [68] (Fig. 9.4).

9.4 Pseudopapilledema

9.4.1 Pseudopapilledema: Vitreopapillary Traction

OCT has been useful in distinguishing other causes of pseudopapilledema, such as vitreopapillary traction, optic nerve head drusen, myelinated nerve fiber layer, and Bergmeister papillae.

Posterior vitreous detachment is a dynamic process characterized by the liquefaction and separation of the posterior vitreous cortex from the inner limiting membrane of the retina. Proliferative disorders, such as the development of premacular membranes, and tractional disorders, such as macular hole formation can result from faulty separation at this interface. If the vitreous partially or anomalously separates from the internal limiting membrane, it can lead to persistent adhesion and even traction on posterior pole structures [69].

Vitreomacular traction syndrome, a result of a partially or anomalously separated vitreous face, is a well-known clinical entity that has been well described in the literature. In 1954, Schepens used the term pseudopapilledema when he demonstrated

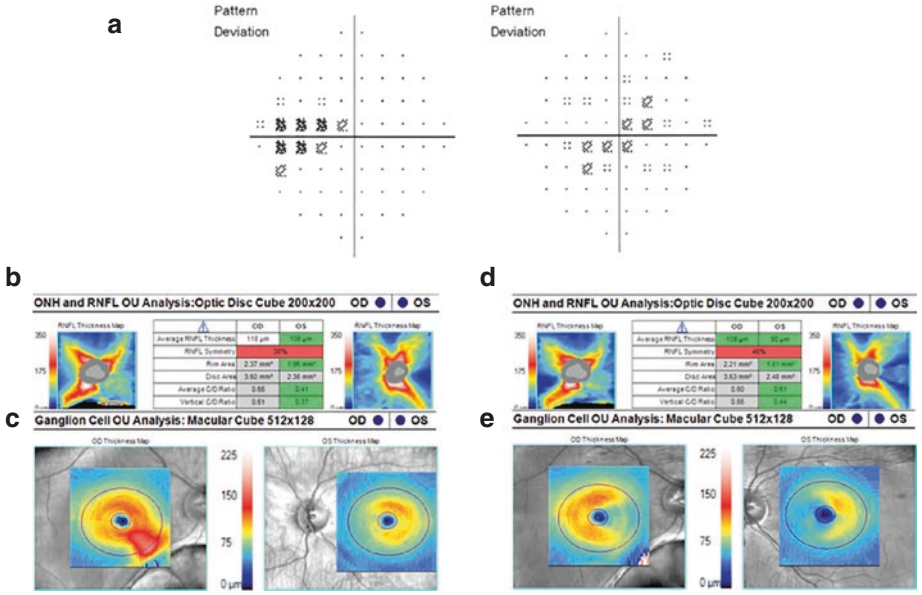

Fig. 9.4 A 19-year-old woman presented with 1 month of bilateral blurred vision, photophobia and a central scotoma after traveling abroad and ingesting methanol in local made liquor and requiring hospitalization for methanol toxicity. Visual fields showed bilateral ceocentral defects (**a**). OCTs of the RNFL and ganglion cell layer complex (GCC) were unremarkable (**b**, **c**). At her 8 month follow-up, there was some mild temporal RNFL thinning OU (**d**) and binasal GCC thinning (**e**). The selective involvement of the papillomacular bundle fibers is common in toxic optic neuropathies and represents damage to the small caliber axons rich in mitochondria

the histopathology of partially detached vitreous at the optic nerve head, usually in the context of co-existing retinal disease [70], such as proliferative diabetic retinopathy [71], central retinal vein occlusion [72], and non-arteritic ischemic optic neuropathy [73]. Using slit lamp biomicroscopy and ultrasonography, Katz and Hoyt observed peripapillary and intrapapillary hemorrhage in 8 young patients with mildly dysplastic discs and persistent vitreopapillary traction, postulating that transmitted forces traumatized disc vessels [74]. In addition, Wisotsky et al. demonstrated in two patients that vitreopapillary traction could cause highly elevated optic discs with blurring of the margins [75].

In 2006, Hedges et al. demonstrated by OCT that persistent vitreopapillary traction could occur as an isolated phenomenon, in the absence of proliferative fibrocellular membranes or vascular insult [76]. Tractional forces from vitreous adhesion on the optic nerve alone were sufficient in causing optic disc elevation, obscured disc margins, and peripapillary hemorrhage in these patients [76]. Vitreopapillary traction has even been shown to cause focal disc leakage on fluorescein angiography [77]. When occurring bilaterally, vitreopapillary traction can be confused with papilledema, potentially leading to costly and invasive diagnostic procedures and even unnecessary treatment [77] (Fig. 9.5).

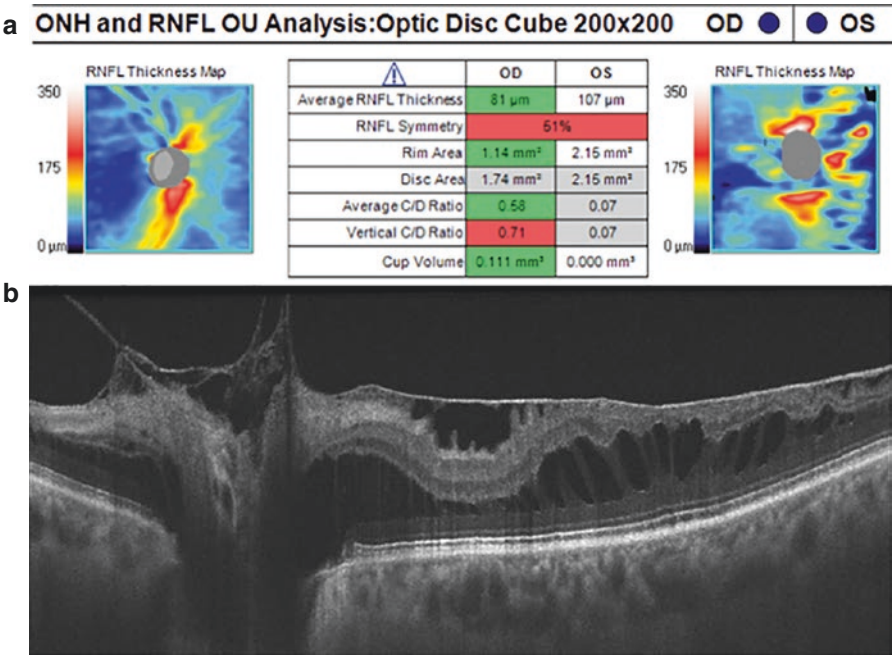

Fig. 9.5 A 74-year-old man was referred for transient flashes of color in the left eye. Automated perimetry testing showed minimal temporal enlargement of the bilind spot with no other visual field loss. Dilated funduscopic examination showed optic disc edema. OCT of the RNFL showed mild disc edema in the left eye (**a**). OCT through the macular and optic nerve of the left eye showed vitreopapilllary and vitreomacular traction (**b**)

9.4.2 Pseudopapilledema: Optic Nerve Head Drusen

Optic nerve head drusen (ONHD) are calcified hyaline deposits and have been associated with small, crowded optic discs [78]. Histopathologically, they are associated with elevation of the optic nerve head, compression of optic nerve fibers, disc hemorrhages, and juxtapapillary retinal scarring [79]. Several predisposing factors for the development of ONHD have been proposed, including a small scleral canal, altered axoplasmic transport, and abnormal vasculature [80].

When ONHD are superficially located on the nerve, they can be recognized as refractile deposits. When they are buried within the optic nerve head, however, they can be much more difficult to identify by ophthalmoscopy alone. Further, they can elevate the optic nerve head and obscure the margins of the optic disc. It is estimated that in approximately 2/3 to 4/5 of cases, ONHD occurs bilaterally [80]. In these cases, ONHD can simulate papilledema. This pseudopapilledema secondary to ONHD is typically benign, whereas true papilledema requires emergent work-up for a potentially life-threatening condition. Thus, differentiating true optic disc edema caused by papilledema or other optic neuropathies is crucial for the ophthalmologist.

Various methods have been used to study buried ONHD, including B-scan ultrasonography, fluorescein angiography, computerized tomography, and fundus autofluoresence [81]. Currently, B-scan ultrasonography is the gold standard in the clinical evaluation of ONHD. Although useful, B-scan ultrasonography necessitates a skilled ultrasonographer and interpreter, and is not always available. Fluorescein angiography is also not readily available and may not be compatible for patients with allergies to shellfish and iodine, which cross react with fluorescein dye. While fundus autofluorescence is a non-invasive way to diagnose ONHD, buried drusen may be missed using this modality. Ophthalmologist are unlikely to subject their patients to radiation to diagnose ONHD with a computerized tomography. OCT, however, is a widely available and has been shown to give information regarding the size, structure, and location of ONHD within the optic disc.

Thinning of the RNFL OCT is often associated with optic atrophy, and thickening of the RNFL OCT is often associated with optic disc edema [82]. However, both ONHD and optic disc edema can present with either RNFL thinning or RNFL thickening on OCT [83]. Therefore, the presence or absence of RNFL thinning or thickening alone does not help the clinician distinguish between ONHD and optic disc edema [84].

Savini et al. examined 9 patients with optic disc edema due to various causes. In addition to noting a significant increase in the mean RNFL thickness in all optic nerve quadrants in patients with optic disc edema, they described a triangular-shaped hyporeflective subretinal space above the retinal pigment epithelium, possibly representing subretinal fluid, with the widest part of the triangle abutting the optic nerve head and the tapered apex pointing away. They hypothesized that swelling induced by the optic disc edema could produce an upward traction producing a subretinal space with the hydrostatic forces overcoming osmotic forces [28].

Expanding on this idea of subretinal hyporeflective space, Johnson et al., used OCT images to examine the qualitative and quantitative differences between ONHD and optic disc edema. They found that patients with ONHD tended to have an elevated optic nerve head with a “lumpy bumpy” internal optic nerve contour, a rapid and abrupt decline in subretinal hyporeflective space with a normal thickness at the 2.0 mm radius, and normal or mildly increased RNFL thickness with the nasal RNFL being less than 86 μm. Patients with optic disc edema, on the other hand, had an elevated optic nerve head with a smooth internal contour, a recumbent “lazy V” pattern of the subretinal hyporeflective space with an increased thickness at the 2.0 mm radius, and an increased RNFL thickness with a nasal RNFL greater than 86 μm. They found a nasal RNFL thickness greater than 86 μm has 80% specificity and a subretinal hyporeflective space thickness greater than 169 μm at 2.0 mm radius has 90% specificity in differentiating between optic disc edema and ONHD [81].

Using SD-OCT, Lee et al. found ONHD to be focal, hyperreflective subretinal masses with distinct margins. They found the RNFL to be deformed with high reflectance and the ONHD to be beneath the outer nuclear layer and on the retinal pigment epithelium. They proposed that the increased thickness and deposition of axonal transport materials in the RNFL in optic disc edema could increase peripapillary RNFL reflectance and induce shadowing of the

underlying retinal layers, mimicking subretinal fluid space rather than representing it. Like Johnson et al., they found RNFL thickness in the nasal section to be a good differential marker for optic disc edema from ONHD, with a thinner cut-off value of 78 μm [84].

Enhanced depth imaging OCT (EDI-OCT), a technique developed to give superior imaging quality of the deeper structures of the retina and optic nerve head, has also shown useful in detecting ONHD. Merchant et al., in an analysis of 34 patients with clinically visible or suspected ONHD based on ophthalmoscopy or optic disc stereophotography, EDI OCT had a significantly higher ONHD detection rate than B-scan ultrasound [85] (Fig. 9.6).

9.4.3 Pseudopapilledema: Bergmeister's Papilla and Myelinated Nerve Fiber Layer

OCT can help characterize other conditions causing pseudopapilledema. In cases of myelinated retinal nerve fiber layer, OCT can show significant hyper-reflectivity and increased thickness of the RNFL in the area of the myelinated fibers [86, 87]. The recent use of wide field three-dimensional swept source OCT (SS-OCT), which utilizes better sensitivity with imaging depth and longer imaging range, has enabled enhanced imaging of vitreous and vitreo-retinal interface. SS-OCT can offer superior resolution of vitreo-retinal entities, such as Bergmeister's papillae that may simulate papilledema [88] (Fig. 9.7).

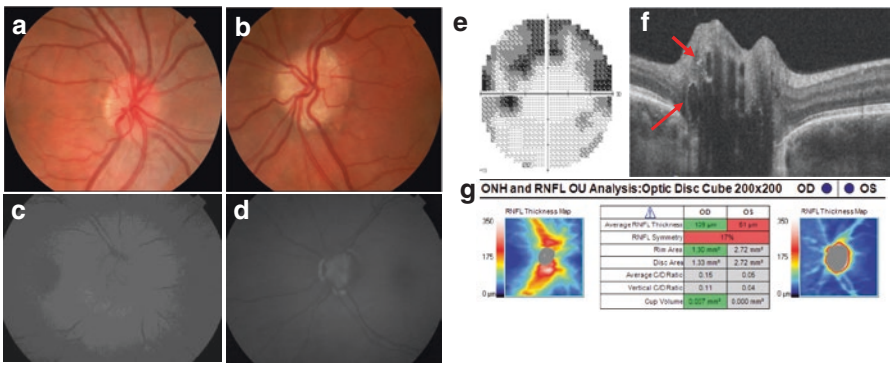

Fig. 9.6 A 16-year-old woman was referred for left visual field loss. On examination, visual acuities were 20/20 in both eyes, there was no afferent papillary defect, and color vision was preserved. The optic discs were crowded in both eyes (**a**, **b**) with multiple optic nerve head drusen (ONHD) in the left eye (**b**). Fundus auto-fluorescence was unremarkable in the right eye (**c**) and revealed numerous round lesions with hyper auto-fluorescence on the optic nerve head in the left eye corresponding with ONHD (**d**). Visual fields showed superior arcuate defect in the left eye (**e**). OCT through the optic nerve showed multiple rings of hyper-reflectivity with internal hyporeflectivity corresponding with the ONHD (**f**). OCT of the RNFL showed thinning superiorly and inferiorly in the left eye (**g**)

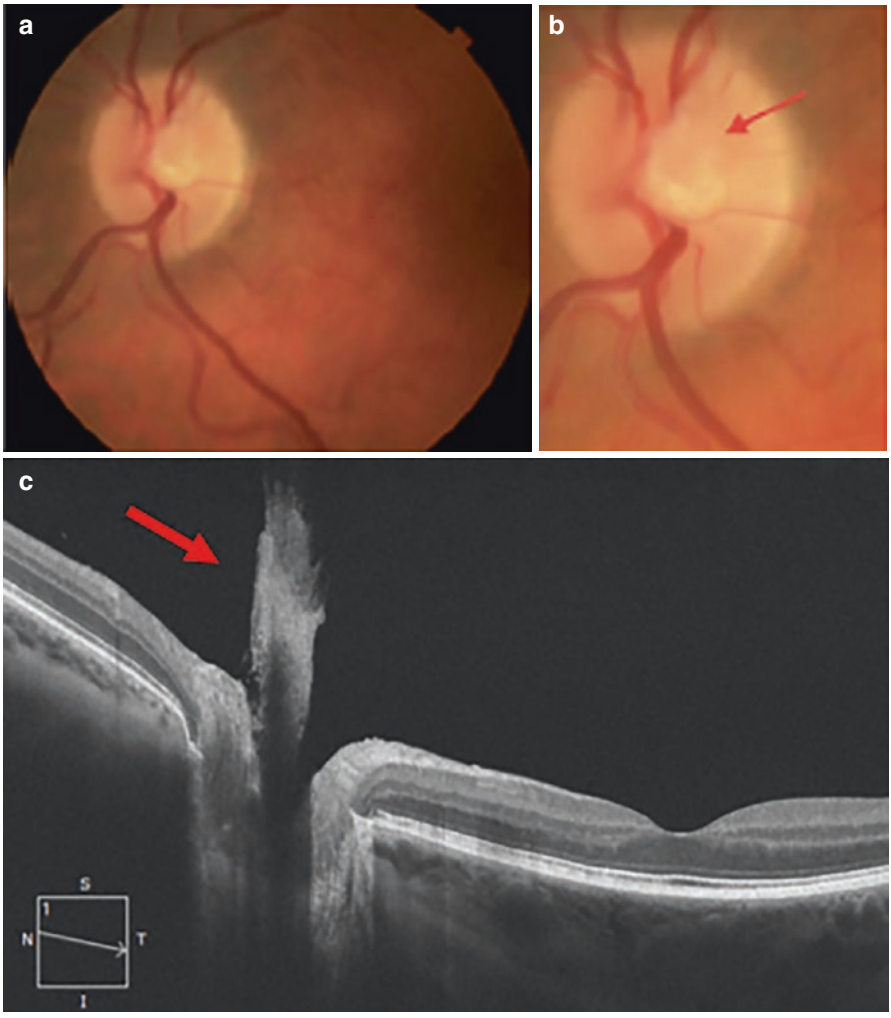

Fig. 9.7 A 43-year-old woman was referred for pain in her left eye. Incidentally, a small tuft of tissue was visualized at the optic disc (**a**, **b**) and appeared to be continuous with the optic disc on OCT (**c**), consistent with Bergmeister papillae

References

1. Von Graefe A. Ueber Komplikation von Sehnervenentzundung mit Gehirnkrankheiten. Arch F Ophth. 1860;7:58–71.
2. Paton L, Holmes G. The pathology of papilledema. Brain. 1911;33:289–432.
3. Fry WE. The pathology of papilledema. Am J Ophthalmol. 1931;14:874–83.
4. Hedges TR. A correlative study of orbital vascular and intracranial pressure in the rhesus monkey. Trans Am Ophthalmol Soc. 1963;61:589–637.
5. Tso MO, Hayreh SS. Optic disc edema in raised intracranial pressure III: a pathologic study of experimental papilledema. Arch Ophthalmol. 1977;95:1448–57.

6. Samuels B. Histopathology of papilledema. Am J Ophthalmol. 1938;21:1242–8.
7. Hoye VJ III, Berrocal AM, Hedges TR III, Amaro-Quireza ML. Optic coherence tomography demonstrates subretinal macular edema from papilledema. Arch Ophthalmol. 2001;119:1287–9.
8. Morris AT, Sanders MD. Macular changes resulting from papilloedema. Br J Ophthalmol. 1980;64:211–6.
9. Corbett JJ, Jacobson DM, Mauer RC, Thompson HS. Enlargement of the blind spot caused by papilledema. Am J Ophthalmol. 1988;105:261–5.
10. Gittinger JW Jr, Asdourian GK. Macular abnormalities in papilledema from pseudotumor cerebri. Ophthalmology. 1989;96:192–4.
11. Jamerson SC, Arunagiri G, Ellis BD, Leys MJ. Intravitreal bevacizumab for the treatment of choroidal neovascularization secondary to pseudotumor cerebri. Int Ophthalmol. 2009;29:183–5.
12. Jamison RR. Subretinal neovascularization and papilledema associated with pseudotumor cerebri. Am J Ophthalmol. 1978;85:78–81.
13. Mas AM, Villegas VM, Garcia JM, Acevedo S, Serrrano L. Intravitreal bevacizumab for peripapillary subretinal neovascular membrane associated to papilledema: a case report. P R Health Sci J. 2012;31:148–50.
14. Lee IJ, Maccheron LJ, Kwan AS. Intravitreal bevacizumab in the treatment of peripapillary choroidal neovascular membrane secondary to idiopathic intracranial hypertension. J Neuroophthalmol. 2013;33:155–7.
15. Morse PH, Leveille AS, Antel JP, Burch JV. Bilateral juxtapapillary subretinal neovascularization associated with pseudotumor cerebri. Am J Ophthalmol. 1981;91:312–7.
16. Caballero-Presencia A, Diaz-Guia E, Martinex-Perez M, Lopez-Lopez J. Neo-vascularisation sous-retinienne jiuxtapapillaire bilaterale dans un cas de pseudotumor cerebri. J Fr Ophtalmol. 1986;9:105–10.
17. Sathornsumetee B, Webb A, Hill DL, Newman NJ, Biousse V. Subretinal hemorrhage from a peripapillary choroidal neovascular membrane in papilledema caused by idiopathic intracranial hypertension. J Neuroophthalmol. 2006;26:197–9.
18. Kaeser PF, Borruat FX. Peripapillary neovascular membrane: a rare cause of acute vision loss in pediatric idiopathic intracranial hypertension. J AAPOS. 2011;15:83–6.
19. Troost BT, Sufit RL, Grand MG. Sudden monocular visual loss in pseudotumor cerebri. Arch Neurol. 1979;36:440–2.
20. Martinez MR, Ophir A. Optical coherence tomography as an adjunctive tool for diagnosing papilledema in young patients. J Pediatr Ophthalmol Strabismus. 2011;48:174–81.
21. Karam EZ, Hedges TR. Optical coherence tomography of the retinal nerve fibre layer in mild papilloedema and pseudopapilloedema. Br J Ophthalmol. 2005;89:294–8.
22. Fard MA, Fakhree S, Abdi P, Hassanpoor N, Subramanian PS. Quantification of peripapillary total retinal volume in pseudopapilledema and mild papilledema using spectral-domain optical coherence tomography. Am J Ophthalmol. 2014;158:136–43.
23. Kupersmith MJ, Sibony P, Mandel G, Durbin M, Kardon RH. Optical coherence tomography of the swollen optic nerve head: deformation of the peripapillary retinal pigment epithelium layer in papilledema. Invest Ophthalmol Vis Sci. 2011;52(9):6558–64.
24. Sibony P, Kupersmith MJ, Rohlf FJ. Shape analysis of the peripapillary RPE layer in papilledema and ischemic optic neuropathy. Invest Ophthalmol Vis Sci. 2011;52(11):7987–95.
25. Sibony P, Kupersmith MJ, Honkanen R, Rohlf FJ, Torab-Parhiz A. Effects of lowering cerebrospinal fluid pressure on the shape of the peripapillary retina in intracranial hypertension. Invest Ophthalmol Vis Sci. 2014;55(12):8223–31.
26. Wang JK, Kardon RH, Ledolter J, Sibony PA, Kupersmith MJ, Garvin MK, OCT Sub-Study Committee and the NORDIC Idiopathic. Peripapillary retinal pigment epithelium layer shape changes from acetazolamide treatment in the idiopathic intracranial hypertension treatment trial. Intracranial Hypertension Study Group. Invest Ophthalmol Vis Sci. 2017;58(5):2554–65.
27. Sibony P, Straachovsky M, Honkanen R, Kupersmith MJ. Optical coherence tomography shape analysis of the peripapillary retinal pigment epithelium layer in presumed optic nerve sheath meningiomas. J Neuroophthalmol. 2014;34:130–6.

28. Savini G, Bellusci C, Carbonelli M, Zanini M, Carelli V, Sadun AA, Barboni P. Detection and quantification of retinal nerve fiber layer thickness in optic disc edema using stratus OCT. Arch Ophthalmol. 2006;124:1111–7.
29. Monteiro ML, Afonso CL. Macular thickness measurements with frequency domain-OCT for quantification of axonal loss in chronic papilledema from pseudotumor cerebri syndrome. Eye (Lond). 2014;28:390–8.
30. Perry VH, Lund RD. Evidence that the lamina cribrosa prevents intraretinal myelination of retinal ganglion cell axons. J Neurocytol. 1990;19:265–72.
31. Burkholder BM, Osborne B, Loguidice MJ, Bisker E, Frohman TC, Conger A, Ratchford JN, Warner C, Markowitz CE, Jacobs DA, Galetta SL, Cutter GR, Maguire MG, Calabresi PA, Balcer LJ, Frohman EM. Macular volume determined by optical coherence tomography as a measure of neuronal loss in multiple sclerosis. Arch Neurol. 2009;66:1366–72.
32. Papchenko T, Grainger BT, Savino PJ, Gamble GD, Danesh-Meyer HV. Macular thickness predictive of visual field sensitivity in ischaemic optic neuropathy. Acta Ophthalmol. 2012;90:e463–9.
33. Aggarwal D, Tan O, Huang D, Sadun AA. Patterns of ganglion cell complex and nerve fiber layer loss in nonarteritic ischemic optic neuropathy by Fourier-domain optical coherence tomography. Invest Ophthalmol Vis Sci. 2012;53:4539–45.
34. Larrea BA, Iztueta MG, Indart LM, Alday NM. Early axonal damage detection by ganglion cell complex analysis with optical coherence tomography in nonarteritic anterior ischaemic optic neuropathy. Graefes Arch Clin Exp Ophthalmol. 2014;252:1839–46.
35. Syc SB, Saidha S, Newsome SD, Ratchford JN, Levy M, Ford E, Crainiceanu CM, Durbin MK, Oakley JD, Meyer SA, Frohman EM, Calabresi PA. Optical coherence tomography segmentation reveals ganglion cell layer pathology after optic neuritis. Brain. 2012;135:521–33.
36. Marzoli SB, Ciasca P, Curone M, Cammarata G, Melzi L, Criscuoli A, Bussone G, D'Amico D. Quantitative analysis of optic nerve damage in idiopathic intracranial hypertension (IIH) at diagnosis. Neurol Sci. 2013;34(Suppl 1):S143–5.
37. Optical Coherence Tomography Substudy Committee, NORDIC Idiopathic Intracranial Hypertension Study Group. Papilledema outcomes from the optical coherence tomography substudy of the idiopathic intracranial hypertension treatment trial. Ophthalmology. 2015;122(9):1939–45.
38. Chen JJ, Thurtell MJ, Longmuir RA, Garvin MK, Wang JK, Wall M, Kardon RH. Causes and prognosis of visual acuity at the time of initial presentation in idiopathic intracranial hypertension. Invest Ophthalmol Vis Sci. 2015;56(6):3850–9.
39. Athappilly G, Garcia-Basterra I, Machado-Miller F, Hedges TR, Mendoza-Santiesteban C, Vuong L. Ganglion cell complex analysis as a potential indicator of early neuronal loss in idiopathic intracranial hypertension. Neuroophthalmology. 2018;43(1):10–7.
40. Hayreh SS. Anterior ischemic optic neuropathy. Arch Neurol. 1981;38:675–8.
41. Hayreh SS. Fluids in the anterior part of the optic nerve in health and disease. Surv Ophthalmol. 1978;23:1–25.
42. Contreras I, Noval S, Rebolleda G, Munoz-Negrete FJ. Follow-up of nonarteritic anterior ischemic optic neuropathy with optical coherence tomography. Ophthalmology. 2007;114:2338–44.
43. Contreras I, Rebolleda G, Noval S, Munoz-Negrete FJ. Optic disc evaluation by optical coherence tomography in nonarteritic anterior ischemic optic neuropathy. IOVS. 2007;48:4087–92.
44. Bellusci C, Savini G, Carbonelli M, Carelli V, Sadun AA, Barboni P. Retinal nerve fiber layer thickness in nonarteritic ischemic optic neuropathy: OCT characterization of the acute and resolving phases. Graefes Arch Clin Exp Ophthalmol. 2008;246:641–7.
45. Quigley HA, Miller NR, Green WR. The pattern of optic nerve fiber loss in anterior ischemic optic neuropathy. Am J Ophthalmol. 1985;100:769–76.
46. Traustason OI, Feldon SE, Leemaster JE, Weiner JM. Anterior ischemic optic neuropathy: classification of field defects by Octopus automated static perimetry. Graefes Arch Clin Exp Ophthalmol. 1988;226:206–12.

47. Hayreh SS, Zimmerman MB. Visual field abnormalities in nonarteritic anterior ischemic optic neuropathy: their pattern and prevalence at initial examination. Arch Ophthalmol. 2005;23:1554–62.
48. Hayreh SS, Zimmerman MB. Optic disc edema in non-arteritic anterior ischemic optic neuropathy. Graefes Arch Clin Exp Ophthalmol. 2007;245:1107–21.
49. Alasil T, Tan O, Lu ATH, Huang D, Sadun AA. Correlation of Fourier domain optical coherence tomography retinal nerve fiber layer maps with visual fields in nonarteritic ischemic optic neuropathy. Ophthalmic Surg Lasers Imaging. 2008;39:S71–9.
50. Hedges TR III, Vuong LN, Gonzalez-Garcia AO, Mendoza-Santiesteban CE, Amaro-Quierza ML. Subretinal fluid from anterior ischemic optic neuropathy demonstrated by optical coherence tomography. Arch Ophthalmol. 2008;126:812–5.
51. Fernandez-Buenaga R, Rebolleda G, Munoz-Negrete FJ, Contreras I, Casas-Llera P. Macular thickness. Ophthalmology. 2009;116:1587–1587.e3.
52. Erlich-Malona N, Mendoza-Santiesteban CE, Hedges TR 3rd, Patel N, Monaco C, Cole E. Distinguishing ischaemic optic neuropathy from optic neuritis by ganglion cell analysis. Acta Ophthalmol. 2016;94(8):721–6.
53. Miller NR, Arnold AC. Current concepts in the diagnosis, pathogenesis and management of nonarteritic anterior ischaemic optic neuropathy. Eye. 2015;29:65–79.
54. Ho JK, Stanford MP, Shariati MA, Dalal R, Liao YJ. Optical coherence tomography study of experimental anterior ischemic optic neuropathy and histologic confirmation. Invest Ophthalmol Vis Sci. 2013;54:5981–8.
55. Wright-Mayes E, Cole ED, Dang S, Novais EA, Vuong L, Mendoza-Santiesteban C, Duker JS, Hedges TR 3rd. Optical coherence tomography angiography in non-arteritic anterior ischemic optic neuropathy. J Neuroophthalmol. 2017;37(4):358–64.
56. Song Y, Min JY, Mao L, Gong YY. Microvasculature dropout detected by the optical coherence tomography angiography in nonarteritic anterior ischemic optic neuropathy. Lasers Surg Med. 2018;50(3):194–201.
57. Barboni P, Savini G, Valentino ML, et al. Retinal nerve fiber layer evaluation by optical coherence tomography in Leber's hereditary optic neuropathy. Ophthalmology. 2005;112:120–6.
58. Zhang Y, Huang H, Wei S, et al. Characterization of macular thickness changes in Leber's hereditary optic neuropathy by optical coherence tomography. BMC Ophthalmol. 2014;14:105.
59. Savini G, Barboni P, Valentino ML, et al. Retinal nerve fiber layer evaluation by optical coherence tomography in unaffected carriers with Leber's hereditary optic neuropathy mutations. Ophthalmology. 2005;112:127–31.
60. Hedges TR, Gobuty M, Manfreddy RA, Erlich-Malona N, Monaco C, Mendoza-Santiesteban CE. The optic coherence tomography profile of Leber hereditary optic neuropathy. Neuroophthalmology. 2016;40(3):107–12.
61. De Rojas JO, Rasool N, Chen RW, Horowitz J, Odel JG. Optical coherence tomography angiography in Leber hereditary optic neuropathy. Neurology. 2016;87(19):2065–6.
62. Matsuzaki M, Hirami Y, Uyama H, Kurimoto Y. Optic coherence tomography angiography changes in radial peripapillary capillaries in Leber hereditary optic neuropathy. Am J Ophthalmol Case Rep. 2018;9:51–5.
63. Barboni P, Savini G, Cascavilla ML. Early macula retinal ganglion cell loss in dominant optic atrophy: genotype-phenotype correlation. Am J Ophthalmol. 2014;158(3):62–636.
64. Moura F, Monteiro M. Evaluation of retinal nerve fiber layer thickness measurements using optical coherence tomography in patient with tobacco-alcohol-induced toxic optic neuropathy. Indian J Ophthalmol. 2010;58(2):143–6.
65. Kee C, Hwang JM. Optical coherence tomography in a patient with tobacco-alcohol amblyopia. Eye (Lond). 2008;22(3):469–70.
66. Fujihara M, Kikuchi M, Kurimoto Y. Methanol-induced retinal toxicity patient examined by optic coherence tomography. Jpn J Ophthalmol. 2006;50:239–41.
67. Eells JT, Henry MM, Lewandowski MF, Seme MT, Murray TG. Development and characterization of a rodent model of methanol induced retinal and optic nerve. Neurotoxicology. 2000;21:321–30.

68. Klein KA, Warren AK, Baumal CR, Hedges TR III. Optical coherence tomography findings in methanol toxicity. Int J Retina Vitreous. 2017;3:36.
69. Sebag J. Anatomy and pathology of the vitreo-retinal interface. Eye. 1992;6(6):541–52.
70. Schepens CL. Clinical aspects of pathologic changes in the vitreous body. Am J Ophthalmol. 1954;38:8–21.
71. Kroll P, Weigrand W, Schmidt J. Vitreopapillary traction in proliferative diabetic vitreoretinopathy. Br J Ophthalmol. 1999;83:261–4.
72. Rumelt S, Karatas M, Pikkel J, Majlin M, Ophir A. Optic disc traction syndrome associated with central retinal vein occlusion. Arch Ophthalmol. 2003;121:1093–7.
73. Modarres M, Sanjari MS, Falavarjani KG. Vitrectomy and release of presumed epipapillary vitreous traction for treatment of nonarteritic anterior ischemic optic neuropathy associated with partial posterior vitreous detachment. Ophthalmology. 2007;114(2):340–4.
74. Katz B, Hoyt WF. Intrapapillary and peripapillary hemorrhage in young patients with incomplete posterior vitreous detachment: signs of vitreopapillary traction. Ophthalmology. 1995;102:349–54.
75. Wisotsky BJ, Magat-Gordon CB, Puklin JE. Vitreopapillary traction as a cause of elevated optic nerve head. Am J Ophthalmol. 1998;126:137–9.
76. Hedges TR, Flattem NL, Bagga A. Vitreopapillary traction confirmed by optical coherence tomography. Arch Ophthalmol. 2006;124(2):349–54.
77. Houle E, Miller NR. Bilateral vitreopapillary traction demonstrated by optical coherence tomography mistaken for papilledema. Case Rep Ophthalmol Med. 2012;2012:682659.
78. Lam BL, Morais CG Jr, Pasol J. Drusen of the optic disc. Curr Neurol Neurosci Rep. 2008;8:404–8.
79. Friedman AH, Gartner S, Modi SS. Drusen of the optic disc: a retrospective study in cadaver eyes. Br J Ophthalmol. 1975;59:413–21.
80. Auw-Haedrich C, Staubach F, Witschel H. Major review: optic disk drusen. Surv Ophthalmol. 2002;47:515–32.
81. Johnson LN, Diehl ML, Hamm CW, Sommerville DN, Petroski GF. Differentiating optic disc edema from optic nerve head drusen on optical coherence tomography. Arch Ophthalmol. 2009;127:45–9.
82. Katz BJ, Pomeranz HD. Visual field defects and retinal nerve fiber layer defects in eyes with buried optic nerve drusen. Am J Ophthalmol. 2006;141:248–53.
83. Roh S, Noecker RJ, Schuman JS, Hedges TR III, Weiter JJ, Mattox C. Effect of optic nerve head drusen on nerve fiber layer thickness. Ophthalmology. 1998;105:878–85.
84. Lee KM, Woo SJ, Hwang JM. Differentiation of optic nerve head drusen and optic disc edema with spectral domain optical coherence tomography. Ophthalmology. 2011;118:971–7.
85. Merchant KY, Su D, Park SC, Qayum S, Banik R, Liebmann JM, Ritch R. Enhanced depth imaging optical coherence tomography of optic nerve head drusen. Ophthalmology. 2013;120:1409–14.
86. Salvatore S, Iannetti L, Fragiotta S, Vingolo EM. Optical coherence tomography and myelinated retinal nerve fibers: anatomical description and comparison between time-domain and spectral domain OCT. Minerva Oftalmol. 2011;53:31–8.
87. Nourinia R, Behdad B, Montahaei T. Optical coherence tomography findings in a patient with myelinated retinal nerve fiber layer. J Ophthalmic Vis Res. 2013;8:280–1.
88. Liu JJ, Witkin AJ, Adhi M, Grulkowski I, Kraus MF, Dhalla AH, Lu CD, Hornegger J, Duker JS, Fukimoto JG. Enhanced vitreous imaging in healthy eyes using swept source optical coherence tomography. PLoS One. 2014;9(7):e102950.